JOURNAL OF MATERIALS SCIENCE **39** (2004) 2199–2204

Carbon nanotubes and nanocrystals in methane combustion and the environmental implications

L. E. MURR, J. J. BANG, D. A. LOPEZ, P. A. GUERRERO, E. V. ESQUIVEL
Department of Metallurgical and Materials Engineering, The University of Texas at El Paso, El Paso, TX 79968, USA

A. R. CHOUDHURI, M. SUBRAMANYA
Department of Mechanical and Industrial Engineering, The University of Texas at El Paso, El Paso, TX 79968, USA

M. MORANDI
School of Public Health, The University of Texas Health Science Center, Houston, TX 77030, USA

A. HOLIAN
Center for Environmental Health Sciences, Department of Pharmaceutical Sciences, University of Montana, Missoula, MT 59812, USA

A variety of combustion-related and thermal plasma techniques, as well as thermal decomposition of hydrocarbons, have been used to produce a wide variety of carbon-based nanoparticles [1, 2]. These have included numerous, novel grades of carbon blacks, fullerenes, and carbon filaments and fibers, particularly carbon nanotubes, which have been produced by decomposition of a hydrocarbon gas over a transition metal since the 1960's, but were only identified around 1991 by Iijima [3] using electron microscopy. Current methods involving aerosol synthesis of carbon nanotubes include arc discharge, laser ablation, and catalytic/decomposition growth for the production of single and multi-walled nanotubes of carbon. Common to these approaches is the generation of particles in the presence of a reactive hydrocarbon species at elevated temperatures (600–1200 °C). In contrast, ordinary combustion flames can naturally form carbon nanoparticles, primarily carbon blacks. Such flames represent a complex chemical environment characterized by steep temperature gradients and concentrations of species. Catalytic decomposition of acetylene (C_2H_2) and methane (CH_4) in the presence of an iron catalyst has been a common methodology for carbon nanotube production [4, 5]. In this letter, the production of a range of carbon nanotubes and nanocrystal particulates, primarily aggregates, by near optimal combustion of pure methane (99.5%) in a laminar methane-air co-flow flame, and evidence for the presence of these carbon nanotubes and nanocrystals in atmospheric aerosols is reported.

Methane was issued from a 0.2 cm-diameter stainless steel tube burner described in detail elsewhere [6]. A narrow range of linear fuel (methane) flow rate/linear air flow rate of (4–5 cm/s)/(50–70 cm/s) was employed to establish a predominantly blue, stable laminar flame with a visible height of ∼7 cm on the burner port.

A thermal precipitator described in detail elsewhere [7] was employed to collect representative combustion products on standard (3 mm) transmission electron microscope (TEM) grids: 100 mesh nickel coated with 60 nm of formvar and carbon. It was located at the top of a cylindrical tube surrounding the flame; approximately 1 m from the flame center. The thermal precipitator has also been employed in the collection of particulate matter, especially nanoparticles, in the indoor and outdoor air of El Paso, TX, USA over a 2-year period [7–9].

Finally, particulate matter with mass median diameter $<2.5\ \mu$m ($PM_{2.5}$) was collected using the Versatile Aerosol Concentration Enrichment System (VACES) [10, 11] in Houston, TX, USA in close proximity to a heavy traffic road. Microdrops ∼1 mm 3 of the $PM_{2.5}$ suspension were pipetted onto the 3 mm, 100 mesh nickel—formvar/carbon-coated grids for examination in the TEM. This technique has been described in more detail in previous studies of particulate matter in water samples using the TEM [12]. In the present studies the TEM was a Hitachi H-8000 analytical TEM operated at an accelerating potential of 200 kV, employing a goniometer-tilt stage; and fitted with a Noran energy-dispersive X-ray spectrometer system.

In performing experiments as outlined above, it was the intention originally to examine variations in soot microparticle agglomeration (assumed to be mostly amorphous carbon or carbonaceous spherules or clusters); and related black carbon forms with small variations in the methane/air flame-related combustion phenomena. What was observed was a variation in crystalline carbon nanostructures, some of which are illustrated in Fig. 1. Fig. 1 shows a series of nanoparticulate/nanocrystal agglomerates observed in the TEM. This series shows the collected agglomerate particulate along with a corresponding, high-magnification, bright-field TEM image. Fig. 1a and b show an agglomerate of primarily carbon nanocrystal polyhedra and other fullerene-related nanoforms. Fig. 1c and d show an agglomerated, complex mixture of carbon nanocrystal polyhedra and other forms, including very prominent nanofibrils which are mostly multi-walled carbon

0022–2461

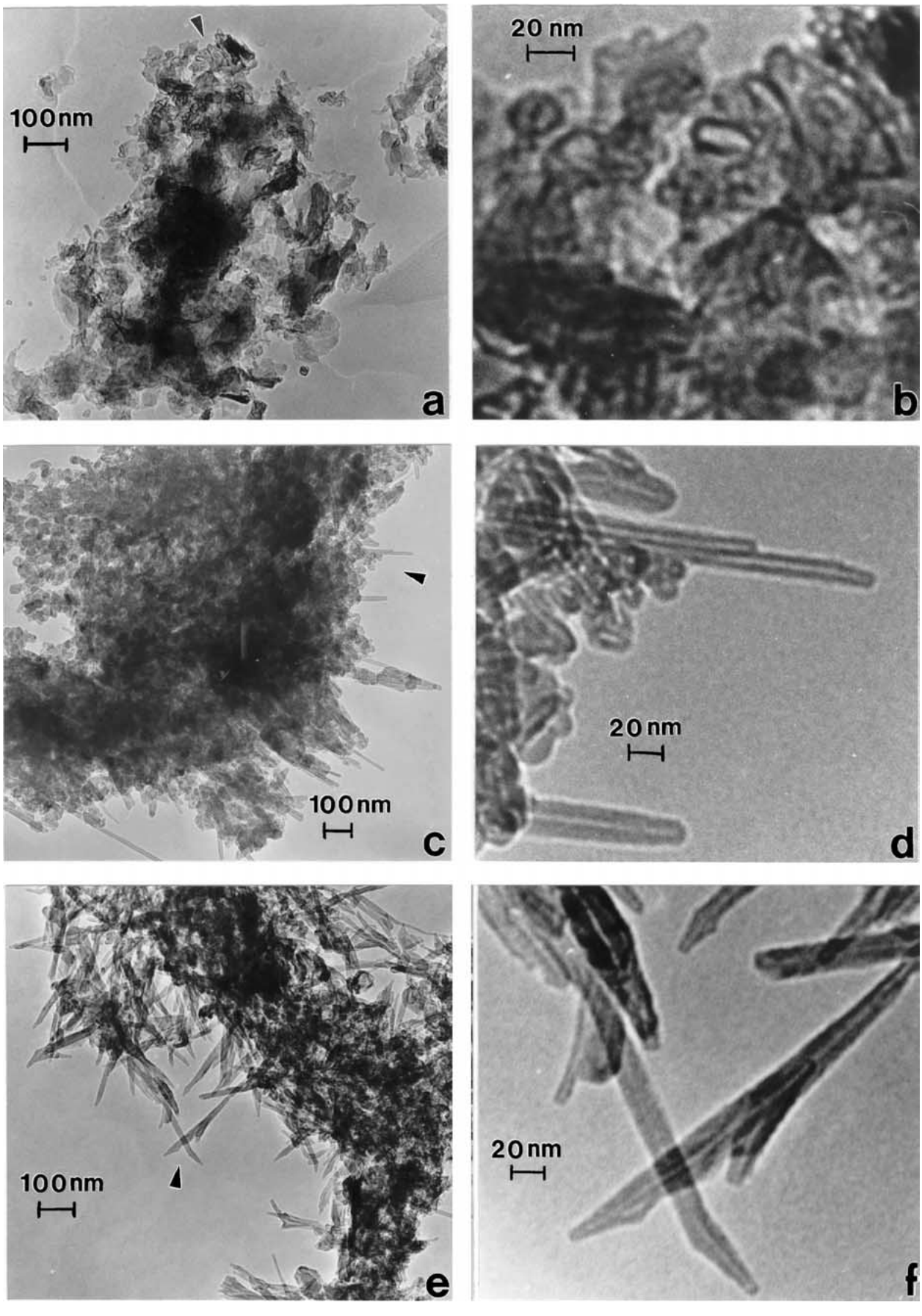

Figure 1 Examples of three different aggregate, particulate, carbon nanocrystal forms collected in a methane/air combustion stream. (a) and (b) show bright-field TEM images of aggregated nanocrystal polyhedra, and a magnified view (b) at arrow in (a). (c) and (d) show nanocrystal polyhedra-nanotube mixture. (d) is a magnified view of (c) at arrow. (e) and (f) show mainly nanotube aggregate. (d) is a magnified view of (e) at arrow.

nanotubes having diameters ranging from 10 to 20 nm. As shown in Fig. 1d the nanotubes exhibit symmetrical and asymmetrical caps. Nanotubes with asymmetrical, cone-like caps are also shown prominently in the magnified view of nanotube agglomerates shown in Fig. 1f. The agglomerated carbon nanocrystals shown in Fig. 1e exhibits primarily nanotubes, somewhat more irregular than the straight, uniform nanofibrils shown in Fig. 1c and d. Some other carbon nanocrystal forms are contained in the aggregated particulate shown in Fig. 1c.

The variations in carbon nanotubes and other nanoforms, and their complex intermixing or agglomeration are reflected in variations in the selected-area electron diffraction (SAED) patterns which are shown in Fig. 2a–c; corresponding to the bright-field image sequences shown in Fig. 1. Fig. 2d shows an energy-dispersive X-ray spectrum corresponding to Fig. 1c, and very typical for all of the collected carbon nanoparticulate agglomerates shown in Fig. 1. The Ni peaks (shown dark shaded) represent the Ni grid mesh and act as an internal, elemental calibration. The S peak is characteristic of most hydrocarbon fuel contaminants. It might be noted in Fig. 2a–c that reflections corresponding to a carbon layer or d-spacing of 0.34 and 0.17 nm is absent in Fig. 2a, while the 0.34 nm d-spacing is essentially absent in Fig. 2c; corresponding to Fig. 1e and f.

While we have not yet specifically explored the methane/air flame parameters in detail in order to maximize the selectivity towards carbon nanotube or other specific fullerene-related nanoforms, it may be possible to achieve such selectivity, as implicit on comparing

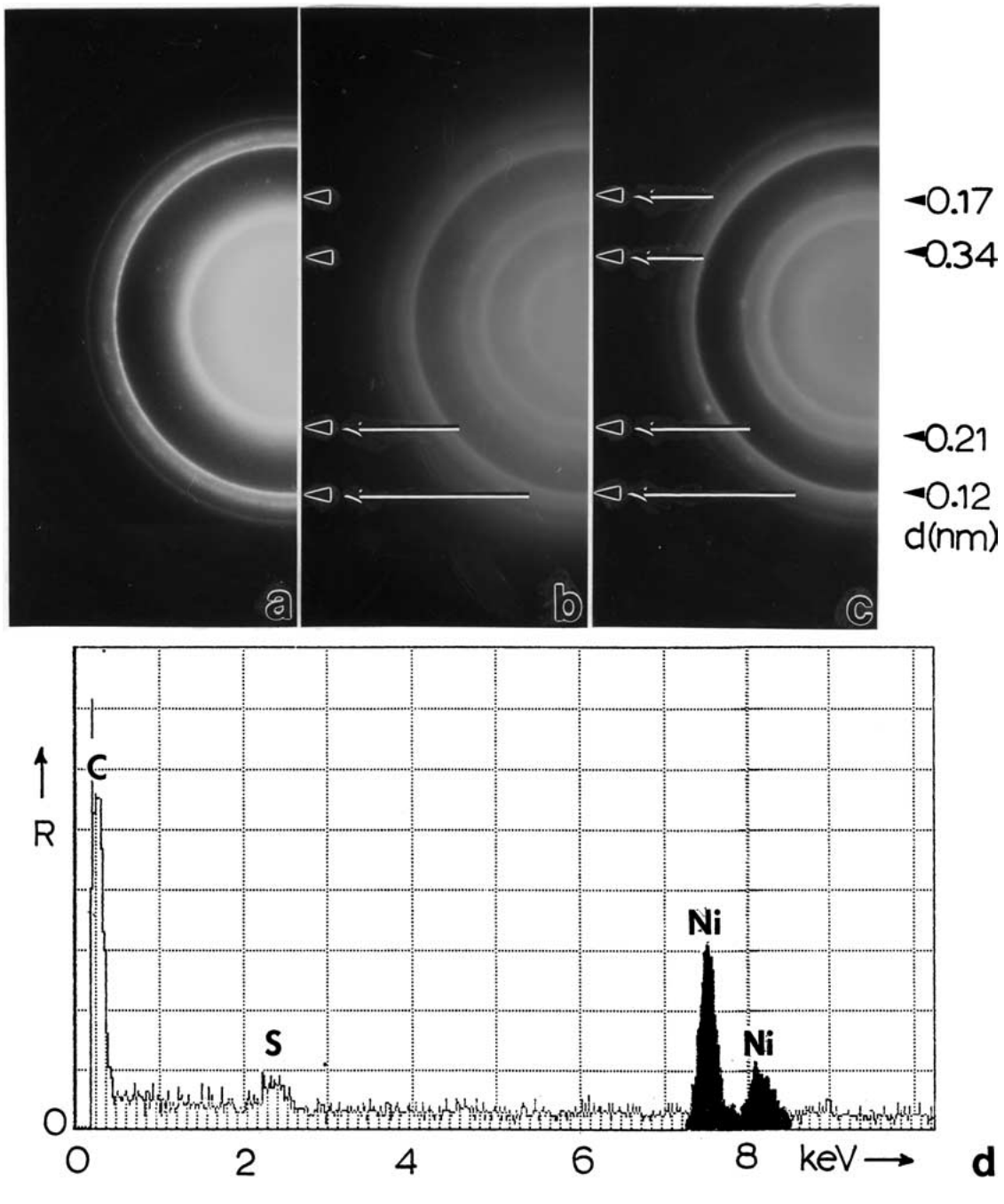

Figure 2 Selected-area electron diffraction (SAED) patterns corresponding to Fig. 1 aggregate sequence. (a), (b) and (c) correspond to Fig. 1a, c, and e, respectively. Carbon interplanar spacing reflections are noted. (d) shows the energy-dispersive X-ray spectrum for Fig. 1c.

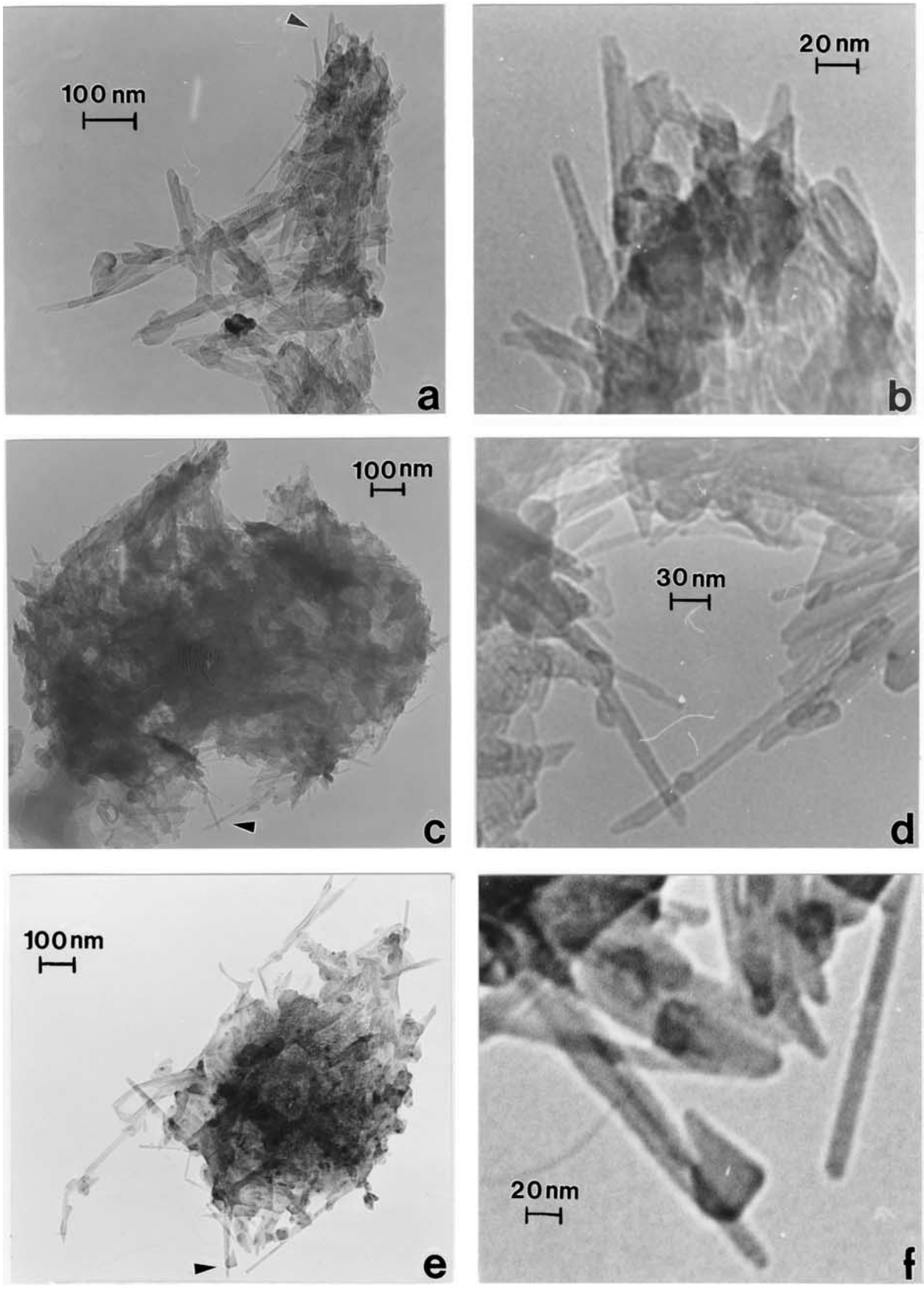

Figure 3 Examples of TEM bright-field images for carbon nanocrystals and nanotubes in airborne particulate-aggregates. (a) El Paso, TX, USA air particulate. (b) shows a magnified view at arrow in (a). (c) and (d) show original and magnified image (arrow in (c)) for Houston, TX, USA air particulate. (e) and (f) show 10 000 year-old particulate trapped in a Greenland ice core. (f) shows a magnified image at arrow in (e).

Fig. 1a–f; without seeding the flame with catalyst particles. The production of carbon nanotubes and nanocrystal aggregates in a reasonably efficient burning methane/air flame raises the question of the potential health and environmental implications of such nanoparticle emissions from natural gas (∼96% methane) burning, including gas stoves and heaters in homes, electric power generation plants, and many other industrial processes or combustion process sources.

It is in fact in the environmental context that the real significance of the observations presented in Fig. 1 becomes apparent. For several years we have collected a wide variety of airborne particulate matter by thermal precipitation onto TEM grids [7–9]. In hundreds of samples collected both indoors and outdoors in El Paso, TX, USA, nearly 90% of the particles collected were aggregates, and a similar percentage were crystalline or polycrystalline [9]. Many of these aggregates were originally characterized as complex aggregates of silica or other nanocrystals with carbonaceous matter. A re-examination of these TEM images and their corresponding analytical data in light of the findings illustrated in Figs 1 and 2 have revealed that a very significant fraction of these airborne particles exhibited aggregated carbon nanocrystals and nanotubes as illustrated typically in Fig. 3a and b. Furthermore, $PM_{2.5}$ freshly collected with the VACES in a water suspension, and transferred to 3 mm, coated, TEM grids also contained complex aggregates of carbon nanotubes and other nanocrystal forms intermixed with nanocrystals of silica; as illustrated typically in Fig. 3c and d. In fact, Fig. 3d is very similar in appearance to Fig. 1f.

Chianelli *et al.* [13] recently noted that amorphous, carbonaceous material collected in atmospheric aerosols occurring in heavily polluted areas of Mexico City also contained fullerene-like materials dispersed throughout. They attributed this particulate material to soot production from burning hydrocarbon-based fuels.

Finally, numerous particle aggregates extracted from a 10 000 year-old ice core melt sample (Greenland ice cap, Dye –3, tube No. 1596 at 506 m depth) and observed in the TEM in a manner identical to Fig. 3c and d for freshly collected airborne particulate matter (with drops put on grids in a class 100 clean room environment) [12] also exhibited carbon nanotubes and nanocrystal forms, and an example of these observations is reproduced in the bright-field TEM images of Fig. 3e and f. The corresponding energy-dispersive X-ray spectrum for the particle in Fig. 3e contained a C/Si signal ratio similar to the C/S signal ratio in Fig. 2d, and the SAED pattern was essentially the same as that shown for carbon nanocrystals shown in Fig. 2b. The significance of Fig. 3e and f in contrast to Fig. 3a–d is the implication that carbon nanotubes and nanocrystals have occurred naturally in the atmosphere for at least 10 000 years, and continue to be a prominent component of the particulate matter regime characteristic of the contemporary atmosphere.

The non-optimized combustion of hydrocarbon fuels, both liquid and gaseous, produces recognizable soot or smoke emissions—carbon blacks and complex carbonaceous mixtures—often observed as branched clusters of essentially amorphous carbon or hydrocarbon spherules. These spherules are 20 to 50 nm in diameter; with up to 2000 such spherules forming single, complex particle aggregates; with average, aerodynamic diameters up to 2 μm [14]. However, more optimized combustion may produce complex aggregates comparatively enriched in the nanotubes and other nanocrystal forms which are common observations in airborne particulate matter as shown typically by Fig. 3a–d in this study.

While the lean burning of hydrocarbons yields exceptionally low pollutant emission in the context of visible soot, as well as superior combustion characteristics, it appears from this very preliminary study that there may be considerable production of carbon nanotubes and other nanocrystal forms in the pollution emission regime which is difficult to detect except by observations utilizing transmission electron microscopy. This also requires the collection of these nanoparticles and nanoaggregates in a format suitable for observation and analysis by TEM. Furthermore, the range of combustion characteristics conducive to carbon nanocrystal production has not been established, and must be explored for a number of fuels, including natural gas, because such emissions may have important implications for the health compromising effects associated with exposure to airborne particulate matter; in particular the ultra-fine mode. A recent survey of 27 toxicology studies world-wide concluded that ultrafine particles can enter the body through the skin, by breathing, or by ingestion, leading to inflammation and other toxic reactions [15]. A Chemical and Engineering News (April 28, 2003) [16] summary of an American Chemical Society Symposium on Nanotechnology and the Environment questioned whether nanomaterials are safe, and asserted that, "early results suggest that some nanoparticles, such as carbon nanotubes, may pose health risks."

Acknowledgments

This research was supported by a Mr. and Mrs. MacIntosh Murchison Endowed Chair (L.E.M.), an EPA-Southwest Center for Environmental Research and Policy (SCERP) Program and an EPA-STAR Fellowship Award (J.J.B.). The authors also wish to acknowledge Dr. Costas Sioutas who built and calibrated the VACES used to collect $PM_{2.5}$ samples in Houston, and Dr. Jack Bristol who facilitated the collaboration between UT-El Paso and UT-Houston investigators. We also thank Dr. Rei Rasmussen of the Oregon Graduate Institute for Science and Technology for providing the ice core sample.

References

1. P. M. AJAYAN and T. W. EBBESEN, *Rep. Prog. Phys.* **60** (1997) 1025.
2. T. M. GRUENBERGER *et al.*, Carbon Black, Fullerene, and Carbon Nanotube Production by Thermal Plasmas, in Proc. Gas Phase Formation and Destruction of Carbon Based Nanotubes, Abbaye de Saint Jacut de la Mer, Jan. 28–30 (2003).
3. S. IIJIMA, *Nature* **354** (1992) 56.
4. D. S. BETHUNE *et al.*, *ibid.* **363** (1993) 605.

5. T. GUO, P. NIKOLAEV, A. THESS, D. T. COLBERT and R. E. SMALLEY, *Chem. Phys. Lett.* **243** (1995) 49.
6. M. SUBRAMANYA and A. CHOUDHURI, Infrared Thermographic Image Reconstruction for Flame Structure Measurements, in Proc. 1st Intl. Energy Conversion Engr. Conf., Portsmouth, VA, AIAA Paper No. 2003-0335 (2003).
7. J. J. BANG, E. A. TRILLO and L. E. MURR, *J. Air Waste Managmt. Assoc.* **53** (2003) 227.
8. J. J. BANG and L. E. MURR, *J Mater. Sci. Lett.* **21** (2002) 361.
9. *Idem.*, *JOM* **54** (2002) 28.
10. S. KIM, P. A. JAQUES, J. R. FROINES and C. SIOUTA, *J. Aerosol Sci.* **32** (2001) 281.
11. S. KIM, P. A. JAQUES, M. C. CHANG, T. BARONE, C. XIONG, S. K. FRIEDLANDER and C. SIOUTAS, *ibid.* **32** (2001) 1299.
12. L. E. MURR and K. KLOSKA, *Water Res.* **10** (1976) 469.
13. R. R. CHIANELLI, M. J. YACAMAN, J. ARENAS and F. ALDAPE, *J. Hazardous Sub. Res.* **1** (1998) 1.
14. K. A. KATRINAK, P. REZ, P. R. PERKES and P. R. BUSECK, *Environ. Sci. Tech.* **27** (1993) 539.
15. C. STUART, Survey Finds the Smaller the Size, the Bigger the Possible Risks, <http://www.smalltimes.com/document_display.cfm?document_id=586> (2003).
16. R. DAGANI, *Chem. Engr. News* **81**(17) (2003) 30.

Received 19 August
and accepted 10 October 2003